

PROJECT DESCRIPTION

HAWAIIAN OCEAN MIXING EXPERIMENT (HOME): FARFIELD PROGRAM

HAWAIIAN TIDAL ENERGY BUDGET

Principal Investigators: Alan Chave, Bruce Cornuelle, Brian Dushaw,
Jean Filloux, Bruce Howe, Douglas Luther, Walter Munk,
Robert Pinkel, and Peter Worcester (Program Leader)
Collaborator: Gary Egbert

1. GOALS

It is widely believed that the topic of ocean tides went to bed with the Victorians. But TOPEX/POSEIDON (T/P) altimetry and ocean acoustic tomography have brought a new dimension to the subject. We propose to measure the energy budget of the farfield barotropic and low-mode baroclinic tides for the Hawaiian Ridge with sufficient precision to quantify the tidal power dissipated in the nearfield of the Ridge. The data are vital in establishing the barotropic to baroclinic mode conversion which is believed to play an important role in maintaining pelagic turbulence and, more important, the abyssal stratification (Munk and Wunsch 1997, 1998). This tidal energy budget will determine limits on the energy dissipated in the nearfield of the Hawaiian Ridge. The results of these proposed process-oriented studies at Hawaii may be used to better model tidal dissipation and internal-tide radiation in the global ocean. The results have implications for climate modeling (Samelson 1998).

Although the HOME Overview provides a complete discussion of the goals of the research proposed here, it is perhaps worthwhile to reiterate briefly the specific scientific motivation for the Farfield Program.

Tides and the Maintenance of Abyssal Stratification.

The maintenance of the abyssal stratification against upwelling associated with 25 Sverdrups of deep and bottom water formation requires 1900 GW with very large error bars (Munk and Wunsch 1997, 1998). Since the global ocean tidal dissipation is 3500 GW, there is plenty of power available from the tides. It is intriguing that numerical values obtained by totally independent methods should be within a factor of two. Nearly all of the tidal dissipation has been spoken for (since 1919!) by dissipation in the turbulent bottom boundary layer (BBL) in shallow seas, however, and so is unavailable for maintaining the abyssal stratification. The most recent BBL estimates based on T/P altimetry are a little more favorable toward the tides playing a role in the maintenance of the abyssal stratification, however, with significant amounts of tidal dissipation unaccounted for by BBL processes. Egbert (1997) finds 500 GW of M_2 dissipation left unaccounted for by BBL dissipation, giving an upper bound of perhaps 900 GW unaccounted for by BBL dissipation for all constituents. Kantha (personal communication) finds

600 GW. The conclusion drawn by Munk and Wunsch is that tidal dissipation is a significant, although not the only, factor in maintaining the abyssal stratification.

The mixing associated with maintaining the abyssal stratification is conjectured to take place in a few concentrated areas of suitable topography. It is essential to study the energy budget in a mixing area. The Hawaiian Ridge is a favorable location for such an experiment. This is the place where the mode conversion was first measured by tomography (Dushaw *et al.*, 1995) and confirmed by satellite altimetry (Ray and Mitchum 1996, 1997). It is a region in which large internal tidal signals have been seen. Finally, the long, linear ridge is a relatively simple geometry (although with some locally complex bathymetry) far from other potential sources of internal tides that would complicate the interpretation.

Tides and Pelagic Turbulence.

Measurements of microstructure (Cox, Osborn, Gregg, ...) and of tracer release experiments (Ledwell, ...) are associated with a pelagic diapycnal diffusivity of order $k_{PE} = 10^{-5} \text{ m}^2 \text{ s}^{-1}$. The associated global energy dissipation is 200 GW (Munk 1997). Ray and Mitchum's (1996) observations imply a mode-1 internal tide radiation in the far field of the Hawaiian Ridge of 15 GW, using T/P altimetry (Figure F.1). Kantha (personal communication) has extended this to a global estimate of 200-400 GW of global radiation. The fact that these dissipation values are

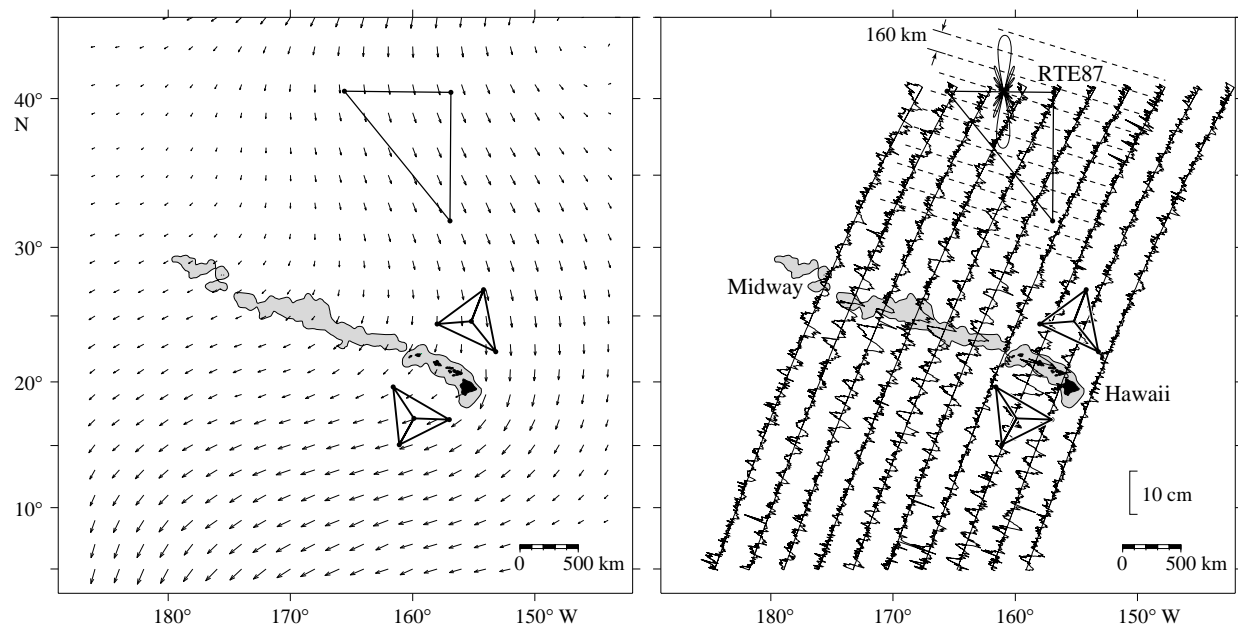


Figure F.1. (Left) M_2 tidal energy flux $\langle p^*u \rangle$, $\langle p^*v \rangle$ computed from the TPXO.3 tidal model. The triangular arrays immediately north and south of the Hawaiian Ridge are the proposed locations of the tomographic measurements. The large triangle to the north of the Hawaiian Ridge is the RTE87 geometry. (Right) High-pass filtered M_2 surface elevations plotted along 10 ascending T/P tracks, from Ray and Mitchum (1996.) The scale is at the lower right. The beam pattern of the northern leg of the RTE87 array for semidiurnal mode-1 baroclinic tidal energy and a cartoon of the internal tide wavefronts deduced from the tomographic data are overlaid on the T/P tracks. Regions in the Hawaiian Ridge with depths shallower than 2000 m are shaded.

similar has led to the proposal that pelagic turbulence is maintained predominantly by the conversion of surface to internal tides over the global ocean ridge structure (Munk 1997). The proposed energy pathway is barotropic tides -> baroclinic tides -> internal waves -> turbulence. There are numerous problems associated with this conjecture, but the fact that the pelagic diffusivity and the intensity of internal waves are astoundingly universal, lying generally within a factor of two under a variety of conditions, speaks for tidal energy as a contribution source more reliable than wind energy. Although not the primary thrust of this proposal, the measurements proposed below will provide significantly improved estimates of the internal tide radiation in the far field of the Hawaiian Ridge and so determine if the energy available from the tides is in fact adequate to support the proposed energy pathway required to maintain pelagic turbulence.

2. TASKS

We propose to subject these speculations to experimental test. One would like to measure in a region of tidal mode conversion (i) the incident and outgoing barotropic tidal energy flux and (ii) the outgoing baroclinic tidal energy flux, separated into the gravest vertical modes. The residual must be dissipated in the nearfield:

$$\text{Astronomical forcing} + \text{Incident barotropic} = \\ \text{Outgoing barotropic} + \text{Outgoing baroclinic} + \text{local dissipation,}$$

assuming that all observed baroclinic energy originates in the mode conversion region. We propose to make these measurements in the vicinity of the Hawaiian Ridge using an array consisting of (Figure F.2):

- (i) four tomographic transceivers to provide precise measurements of barotropic tidal currents and low-mode baroclinic tidal displacements;
- (ii) eight deep ocean horizontal electrometers to complement the tomographic measurements of barotropic tidal currents;
- (iii) eight deep ocean pressure gauges to measure the tidal pressure field; and
- (iv) R/P FLIP to measure the modal content of the baroclinic tidal signal in the farfield.

In order to measure the barotropic and baroclinic tidal energy fluxes on both sides of the Hawaiian Ridge, while minimizing costs, the tomographic array will be deployed twice, first on the north side of the Ridge and then on the south side. Each location will be occupied for approximately four months. R/P FLIP will be moored WSW of the Ridge for 30 days during the time that the tomographic array is deployed in the same area. The horizontal electrometers (HEM) and pressure gauges (Pb) will be deployed both north and south of the Ridge for about 13 months (to ensure clean separation of M_2 from the solar daily variation for the HEMs). The tentative schedule is:

- | | |
|----------------|--|
| October 2000: | Deploy the tomographic array north of the Ridge and all of the HEM and Pb instruments. |
| February 2001: | Recover the tomographic array and redeploy it south of the Ridge. |
| April 2001: | Moor R/P FLIP WSW of the Ridge for 30 days. |
| June 2001: | Recover the tomographic array. |
| November 2001 | Recover the HEM and Pb instruments. |

The measurements of barotropic currents and pressures will be assimilated, together with T/P data and coastal sea level data (see the Historical Data Analysis Program), into a regional numerical model of the tides by G. Egbert. The model results will provide a dynamically consistent interpolation of the tomographic, horizontal electrometer, bottom pressure, T/P, and coastal sea level data, which can then be used to estimate the barotropic tidal energy fluxes and flux convergence with high precision.

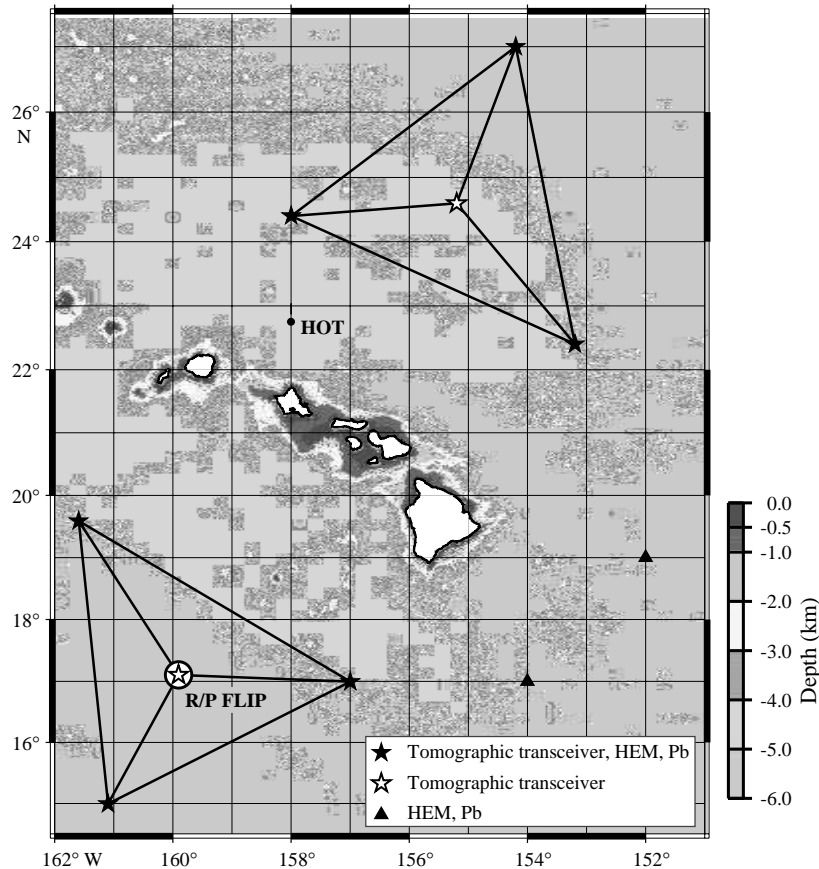


Figure F.2. Map of the Hawaiian Islands with the proposed locations of the tomographic transceivers co-located with the HEM/Pb pairs (solid stars), the tomographic transceivers alone (open stars), the HEM/Pb pairs alone (triangles) and the location where R/P FLIP will be moored for a duration of one month (open circle). The shaded topography is taken from the Smith-Sandwell digital bathymetric dataset.

Required Precision.

The barotropic and baroclinic tidal energy flux divergences must be measured with high precision to provide useful constraints on the dissipation and mixing occurring at the Hawaiian Ridge. A few numbers will help:

Barotropic tidal displacement:	$a = 0.3 \text{ m},$	$c_g = 200 \text{ m/s}$
Baroclinic tidal displacement (mode 1):	$a = 30 \text{ m},$	$c_g = 2 \text{ m/s}$
Barotropic power:	$(1/2) \rho g a^2 c_g =$	10^5 W/m
Baroclinic power:	$(1/2) \rho g a^2 c_g \Delta\rho/\rho =$	10^4 W/m

The total energy flux in the baroclinic tides is then about 15 GW, roughly in accord with the observations of Ray and Mitchum (1996). This is the minimum dissipation, assuming that the radiated internal tides (mode 1) are the only loss. This yields a 10% loss to the barotropic tides, or 90% transmitted energy, 95% transmitted amplitude. Tidal amplitudes therefore need to be measured to considerably better than 5%.

3. BAROTROPIC TIDAL ENERGY FLUX AND FLUX CONVERGENCE

In order to compute the barotropic tidal energy flux components, $\langle p * u \rangle$ and $\langle p * v \rangle$, and the tidal flux convergence around the Hawaiian Islands, both the current and pressure fields are required. The energy fluxes depend sensitively on the phase differences between the two fields. In addition, small errors in the energy flux vectors can lead to large differences in flux convergence estimates, because the convergence represents the (relatively) small difference of large numbers.

Estimates of global tidal current and pressure fields are available from tidal models. Comparison of tidal models with other data types indicates that these models are remarkably accurate away from islands and other significant topography, especially those that have been constrained using sea surface elevations measured by T/P, such as TPXO.2 (Egbert *et al.*, 1994) and TPXO.3. Even the modern models are less accurate near topography and islands, however.

Sea surface elevation is of course directly related to tidal pressure. Filloux *et al.* (1991) compared estimates of tide constituents, obtained from deep ocean pressure gauges in two open ocean experiments (Ocean Storms and BEMPEX) that lasted for approximately one year each in the late 1980's, with constituents taken from Schwiderski's (1979) global tide model. For the seven Ocean Storms pressure gauges (with pressure converted to equivalent sea level height), all situated within a 150 km circle near 47°N, 139°W, the M_2 tide amplitudes exceeded Schwiderski's values by a mean of 1.9 cm (0.4 cm s.d. about the mean), or less than 3% of the amplitude of the M_2 tide, a remarkably close agreement given the probable inaccuracies in the model. A similar comparison of M_2 tide estimates from the five BEMPEX pressure gauges, spread out over roughly 1100 km zonally and 750 km meridionally around 40°N, 163°W, yielded a mean difference of 1.7 cm (0.6 cm s.d.), i.e., the observed amplitudes were 5–9% higher with phase differences of 1-10 degrees.

Comparison of the BEMPEX M_2 tides with a recent update (called TPXO.3) of the Egbert *et al.* (1994) tide model that assimilates T/P tide estimates and deep-sea gauge values (including some from BEMPEX), yields amplitude differences of 0.2 to 1.1 cm (1–4%, with the observed tides still greater) and phase differences of only -1.1 to 0.6 degrees (Dushaw, personal communication). This is not surprising, given that TPXO.3 is constrained to be consistent with a subset of the BEMPEX pressures, but it demonstrates that modern tide models do an excellent job of providing pressure in the open ocean. The issue here, however, is the accuracy of the pressure values near topography, as will be discussed further below.

Model tidal currents have been compared with estimates from two tomographic experiments, the 1987 Reciprocal Tomography Experiment (RTE87) and the 1991–92 Acoustic Midocean Dynamics Experiment (AMODE). To high precision, the difference of reciprocal travel times between two acoustic transceivers gives the average current between the transceivers (Munk *et al.*, 1995). The data collected during RTE87 in the central North Pacific were used to compute the barotropic tides (Dushaw *et al.*, 1995). For the 100-day record length available, the tomographic data provided estimates of barotropic tidal current amplitude and phase that were accurate to a fraction of a mm/s (about 2%) in amplitude and to about 2° in phase (Dushaw *et al.*, 1995, Dushaw *et al.*, 1997). AMODE, located between Puerto Rico and Bermuda, provided a similar opportunity for highly accurate, spatially-filtered observations of the barotropic tides (Dushaw *et al.*, 1996). A comparison of the estimated barotropic tidal currents with the TPXO.2 model currents found excellent agreement *except* in the southern part of the AMODE array, near the Caribbean island arc (Dushaw *et al.*, 1997). The disagreement observed was consistent with spatially coherent errors in the model resulting from the nearby islands and was reflected in the model error bars.

These results suggest that the pressures and currents from modern tidal models constrained by T/P such as TPXO.2 and TPXO.3 are accurate to 10% or better, and might be adequate for calculating barotropic energy flux and flux convergence in open ocean regions, without the need for direct pressure and current observations. As noted above, however, we need tidal amplitudes accurate to considerably better than 5%. Recent results from a preliminary regional tidal model for the Hawaiian Ridge (Egbert, personal communication) show that the currents, energy fluxes, and tidal dissipation at the Ridge are sensitive to different drag parameterizations. Tidal currents parallel to the Ridge decrease by a factor of 3–4 and tidal dissipation increases by a factor of 5–6 when the drag coefficient in the model is increased by an order of magnitude. Further, the AMODE results show unambiguously that near topography and islands, the model's dissipation parameterization, less than perfect topography, and reduced data availability (the island land areas interfere with the altimeter) all lead to a lack of confidence that the TPXO.3 tidal pressure and current fields have the better than 5% accuracy needed to estimate the minimum amount of energy flux divergence that is expected at the Hawaiian Islands. It is conceivable that the tidal models might be improved close to bathymetry using along-track altimetry, rather than just cross-over points, as discussed by Tierney *et al.* (1998), but along track estimates obtained by direct harmonic analysis of altimetry data will not be generally useful for estimating energy fluxes because they will be contaminated by the phase-locked component of the internal tide surface expression (Ray and Mitchum 1997).

Furthermore, the comparison of the K_1 tide observed in BEMPEX with the TPXO.3 model output yields mean amplitude differences of 1.0–1.8 cm (4–8%, with the observed tides always higher) and phase differences of -0.7 to -1.3 degrees (Dushaw, personal communication). Although still not a bad model-data comparison, the suggestion is that the TPXO.3 model is less accurate for constituents other than M_2 . Constituents other than M_2 contribute 30% of the energy dissipated globally by the tides.

Our conclusion is that direct measurements of the tidal currents and pressures are required to determine the barotropic tidal energy flux and flux convergence with adequate precision to construct an energy budget in the vicinity of the Hawaiian Ridge. We propose to use tomographic measurements, augmented by HEM's, to determine the tidal currents and bottom pressure gauges to determine the tidal pressures. The tidal current and pressure data will be used by G. Egbert to constrain a regional numerical model of the barotropic tides that already assimilates T/P measurements of tidal sea-surface height fluctuations. After the direct tidal current and bottom pressure data from the vicinity of the Ridge have been assimilated into the model, it can be used with greater confidence to calculate the barotropic tidal energy flux divergence around the Ridge (and other open ocean topographic features). The TPXO.3 model, based solely on T/P altimetry, shows strong energy flux *around* the southeast end of the Ridge, rather than *across* the Ridge (Figure F.1). One of the first-order questions to be addressed by measurements is whether this model result is correct or an artifact of incorrect assumptions about the dissipation at the Ridge.

Barotropic Currents.

Tomographic Measurements. Worcester, Dushaw, Munk, Howe and Cornuelle propose to prepare an array of four 250-Hz transceivers, with three of the instruments in a triangle and the fourth instrument in the center (Figures F.1 and F.2). All of the transceivers will transmit to all of the other transceivers, so that sum and difference travel times can be formed for all possible acoustic paths. The transceivers will transmit at 3-hr intervals every other day.

The tomographic measurements provide the tidal currents along the acoustic paths with an accuracy of about 2% in amplitude and 2° in phase. Previous comparisons show that current meters cannot determine barotropic tidal currents nearly as well as tomographic measurements. Dushaw *et al.* (1997), Firing's LADCP measurements (personal communication), and many other examples show that the TPXO tidal model currents are accurate in the open ocean to about 10% accuracy, as discussed above, or the value of the model uncertainties. This model may be used to examine the accuracy of previous current meter measurements of tidal harmonic constants. Luyten and Stommel (1991), Dick and Siedler (1985), and Siedler and Paul (1991) report tables of tidal harmonic constants derived from current meters in the open ocean. Scatter plots of these values vs. the TPXO model values (Dushaw *et al.*, 1997) show that the current meter values are often in error by 20–30%. While some of the differences between measured and modeled current may be caused by local topographic influences or the effects of internal tides, the dominant source of error is most likely the excessive noise in the data obtained at single points. Indeed, data obtained from separate deployments of moorings in the Eastern Atlantic at the same location but at different times (6 current meters located throughout the water column) often resulted in tidal amplitudes for the barotropic mode that differed by up to 30%

(Siedler and Paul 1991). If we assume that a well-instrumented, six-element current meter mooring can estimate barotropic tidal harmonic constants to 10% accuracy, then 25 of these moorings (150 current meters) are required to reduce the uncertainty to the 2% available from tomography. A 10% accuracy rate per mooring is probably optimistic, because the baroclinic-tide “noise” near Hawaii is likely to be severe. Further, because an accurate description of the geographical variation of the barotropic tide is one of the main goals of this proposal, data from a current meter array cannot be combined to reduce the uncertainty of the tidal estimates in this \sqrt{N} fashion, unless the moorings are all deployed at one point. For this calculation we assumed that modern current meter measurements are able to avoid current meter stalling such as reported by Luther *et al.* (1991) during BEMPEX, which forced an ad hoc 40% increase in the derived tidal amplitudes before agreement with tidal model and tomographic constants was achieved.

Horizontal Electrometer Measurements. Luther, Chave, and Filloux propose to deploy eight deep ocean horizontal electrometers (HEM's), three each to the north and south of the Hawaiian Ridge collocated with the tomographic arrays and two to the southeast of the Hawaiian Ridge, where the TPXO.3 model shows large fluxes sweeping around the Ridge (Figure F.1). The barotropic tidal currents determined from the HEM's (after using the tomographic tidal currents to calibrate the relation between electric fields and barotropic currents at tidal frequencies) will provide estimates of the barotropic energy flux complementary to that provided using the tomographically-derived currents.

Horizontal electric fields in the ocean are independent of depth and are directly linked to the movement of the entire water column through the earth's stationary magnetic field (Sanford 1971; Chave and Luther 1990). At low frequencies (less than 0.5 cpd), Luther *et al.* (1991) demonstrated with data from BEMPEX the superior capability of horizontal electrometers to measure weak barotropic currents compared to mechanical current meters that tend to stall at low speeds. At the M_2 tidal frequency, Filloux *et al.* (1991) compared currents derived from BEMPEX electrometers with currents from Schwiderski's (1979) model. The electrometer currents averaged 20% (7% s.d.) less than Schwiderski's. Some of the differences are probably due to flaws in the tidal model; these flaws have been fully discussed in the literature on newer models that assimilate T/P data (whereas only coastal and island data were available to Schwiderski).

But some of the differences are likely due to moderate interaction of the tidally-generated electric fields with the seafloor (unlike the case at low frequencies), as discussed by Filloux *et al.* (1991). Since the electrical properties of the seafloor vary little over a distance of a thousand km, we expect to be able to determine a calibration constant by comparison of the tomographically-derived barotropic tidal currents with the electrometer-derived barotropic currents. This calibration will then permit the estimation (to within 5% we believe) of the tidal currents to the southeast of the Hawaiian Island Ridge, outside of the tomographic arrays, with two exceptions. The exceptions are the S_1 and S_2 constituents, at exactly 24 and 12 hours, respectively. The electric fields for these constituents are dominated by “tidal” signals generated in the ionosphere. However, the amplitudes of the barotropic tidal currents at these frequencies can be determined well by interpolation across these frequencies of the tidal response function at neighboring constituents, since the response function is generally quite smooth across each (diurnal and semi-diurnal) tide band (Munk and Cartwright 1966).

Tidal Pressure.

Bottom Pressure Gauges. Luther, Chave, and Filloux propose to deploy eight deep ocean pressure gauges (Pb's) coincident with the HEM's to mitigate the potential inaccuracy of T/P tides (and models assimilating them) near the Hawaiian Island chain, providing the highest accuracy possible for estimating energy fluxes for the major tidal constituents.

The instruments have high resolution, sensitivity and accuracy, except that the DC component is not obtained. The resolution is better than 0.5 mm of water head. The sensors still drift a few 10's of centimeters over long time periods under the strain of deep ocean pressures, but this drift is well characterized by a simple power law formula and is not dependent upon temperature (Filloux *et al.*, 1991).

4. FARFIELD INTERNAL-TIDE RADIATED ENERGY

A low-wavenumber response of the stratification to the incident barotropic wave impinging on the Hawaiian Ridge has been demonstrated by previous tomographic data (Dushaw *et al.*, 1995) and T/P observations (Ray and Mitchum 1996, 1997). Both of these observations show that the low-mode internal tide field is highly anisotropic with dominant propagation away from the Ridge, and that the tidal waves retain spatial and temporal coherence for O(2000 km) and O(6 days) (Figure F.1). As noted above, Ray and Mitchum's observations imply approximately 15 GW of mode-1 energy flux away from the Hawaiian Ridge, suggesting that the Ridge is a significant energy sink for the barotropic tide. The low-mode response may be due to both the extensive regions of super-critical slope on the Hawaiian Ridge and to the insensitivity of the conversion process to topographic variations on scales short compared to the mode-1 length scale (150 km).

We anticipate that sea surface elevation measurements will continue to be available from T/P or a follow-on mission at the time of the proposed experiment, providing information on the mode 1 internal tide fields over the entire Hawaiian Ridge. We do not believe that the data from T/P are adequate by themselves to accurately resolve the tidal energy flux away from the Ridge, however, and that the 15 GW implied by Ray and Mitchum could be significantly in error. One symptom of error is that the T/P results suggest an e-folding scale to the baroclinic waves of about 500 km, while the tomographic data (Dushaw *et al.*, 1995, Dushaw and Worcester, 1998) suggest much longer decay scales. The 10-day sample interval of T/P is a poor way to obtain the tides, and the signals have low signal-to-noise ratios. In addition, because the analysis relies on tidal coherence over three years, the altimetry result is degraded by incoherent components of the field.

The Historical Data Analysis program proposes to analyze data from the principal Hawaii Ocean Time-series (HOT) site at 22.75°N, 158°W, to obtain information about, for example, baroclinic tide energy levels, propagation directions, vertical structure, and the low frequency variation of these quantities. But these "historical" datasets, while providing valuable insight as well as input for model validation, are spatially limited (vertically, as well as the obvious horizontal

limitation) so that it will not be known whether the information they provide is representative of the baroclinic tide signals emanating from the Hawaiian Ridge. Furthermore, the HOT site may not be far enough from the Ridge to be in the "far field." Additional, purposeful observations of the baroclinic tides in the far field are needed. We propose to use a combination of integral tomographic measurements and point measurements to obtain accurate estimates of the baroclinic tidal structure and energy flux away from the Ridge.

Tomographic Measurements.

To high precision, the sum of reciprocal travel times between two acoustic transceivers gives the average sound speed (temperature) along the path (Munk *et al.*, 1995). To our surprise, a phase-locked tidal signal was observed in the sum travel times from RTE87, due to isotherm displacements associated with the internal tide (Dushaw *et al.*, 1995). The observed internal-tide variability was highly anisotropic with evident long time and space coherence. The phase difference between the M_2 and S_2 constituents and the obvious antenna properties of the acoustical array suggested the origin of the internal tide was the Hawaiian Ridge located 2000 km to the south. The estimated energy flux was about 180 W/m at 40° N, although this result cannot be translated to obtain the total baroclinic energy flux away from the Ridge without assuming a decay scale for the baroclinic tides. These results were later confirmed by Ray and Mitchum (1996).

AMODE in the western North Atlantic provided a similar opportunity for highly accurate, spatially-filtered observations of the baroclinic tides (Dushaw and Worcester, 1998). The internal tide observed by the AMODE array is highly temporally and spatially coherent. These tidal signals are phase-locked, with the tidal fits accounting for up to 60% of the high-frequency (> 1 cpd) variance. The phases determined on the various paths are consistent with the 150-km wavelength of the mode-1 semidiurnal internal tide. In addition, no obvious decay of internal tide amplitude away from the continental shelf is evident, although the TOPEX/POSEIDON results of Ray and Mitchum (1996) around Hawaii suggest a 500-km e-folding scale. The pentagonal AMODE acoustical array acted as an antenna with good angular sensitivity.

Recently, the enhanced K_1 and O_1 tidal signals observed in the AMODE data were shown to result from diurnal internal waves of the lowest vertical mode resonantly trapped between the shelf just north of Puerto Rico and the turning latitude at 30° N, a distance of about 1100 km (Dushaw and Worcester, 1998). The data from the AMODE array are consistent with the predicted Airy-function variation with latitude of diurnal internal waves near their turning latitudes. At the K_1 frequency, the ratio of baroclinic energy to barotropic energy is about 30 J/m² to 15 J/m², and similarly for O_1 . Since these baroclinic tides have roughly twice the energy of their barotropic parents, it is evident that energy is stored in the resonating waves. The Hawaiian Ridge topography may well allow for similarly trapped diurnal internal tides and enhanced diurnal amplitudes.

The tomographic array proposed here has been designed to have enough vertical (or modal) and spatial resolution of the outgoing internal-tide field to measure the large-scale, low-vertical-wavenumber, outgoing radiated energy. The variety of upper- and lower-turning depths for the acoustic rays will give adequate resolution for perhaps the first three modes (but dominantly

mode-1). The vertical and horizontal integrating nature of the data is an effective filter against higher-order modes and smaller-scale noise.

The array geometry has been selected to optimize our ability to resolve the baroclinic tidal energy flux as a function of azimuth. The orientations of the multiple acoustic paths with respect to the Ridge axis give good sensitivity as a function of azimuthal angle (Figure F.3). The angular sensitivity of an acoustic path to incident radiation is described by the beam pattern of a line-integral antenna (Urlick, 1983; Dushaw *et al.*, 1995); this beam pattern is equivalent to a sinc filter along one dimension in wavenumber space resulting from the line integration along one dimension in physical space (i.e., a boxcar filter). For the 150-km wavelength associated with the semidiurnal internal tide and a 400-km tomographic path, the 3-dB width of the beam pattern is 20° . The beam patterns are much narrower for modes 2 and 3 at semidiurnal frequencies, because of their shorter wavelengths. At diurnal frequencies, for which the mode-1 wavelength is about 400-km, the beam pattern is quite wide, while for mode-2 the beam pattern width is comparable to the mode-1 semidiurnal beam pattern.

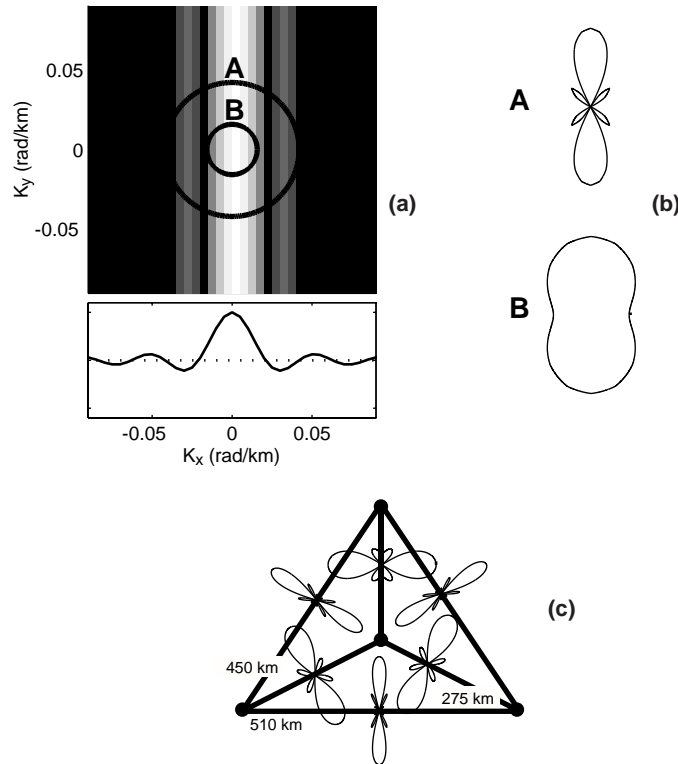


Figure F.3. (a). A zonally-oriented acoustic path of 400-km length gives a sinc filter for zonal wavenumbers and no filter for meridional wavenumbers. (b). The projection of the two-dimensional filter onto semidiurnal wavenumbers **A** is the beam pattern (in polar coordinates), or the response of the line-integral antenna as a function of azimuthal angle, for semidiurnal radiation. The narrow beam pattern shows that the acoustic antenna has high directivity for semidiurnal wavenumbers. For the smaller diurnal wavenumbers **B** the acoustic antenna has less directivity. The proposed acoustic tomography array (c) has been designed to provide for near-complete coverage of the outgoing baroclinic-tide wavenumbers.

Because the tidal variations of acoustic travel time are an average of internal-tide displacement for the wavenumber perpendicular to the acoustic path, the associated tidal potential energy may be directly calculated. The tidal kinetic energy may then be inferred using the theoretically expected ratio of potential to kinetic energy ($(\omega^2 - f^2)/(\omega^2 + f^2) = 0.68$ at 25° N, where ω and f are tidal and inertial frequencies); the energy flux is the total energy density times the mode group velocity (Wunsch, 1975). For the RTE87 tomography triangle, the observed 180 W/m northward energy flux corresponds to 360 MW of northward mode-1 radiation from the 2000-km long Ridge. This estimate represents a lower bound, because the RTE87 triangle was not oriented optimally to measure the baroclinic tides radiated from the Ridge.

The temporally incoherent tidal field can be determined from the acoustic data by examining the residual “tide-like” variability after removing the phase-locked tide. The low-frequency (< 1 cpd) tomographic estimates of current and temperature (and hence the buoyancy frequency) variations provide a measure of the low-frequency variation of the environment through which the internal-tide radiation propagates. The observed low-frequency variations may be used to place limits on the expected incoherent components of the internal-tide radiation. Recent work with the HOT CTD data by Dushaw shows that the phase speeds of the lowest few modes vary by only about 3% (mainly due to mesoscale variability) over the 10 years of the HOT data, however. Thus, incoherence in the low-mode internal tides is more likely caused by variations in the generation conditions, or by mesoscale currents, rather than by buoyancy fluctuations.

Point Measurements. The Farfield integrating measurements are most sensitive to the lowest mode internal tides. A central concern of HOME is the fate of the high mode, small vertical scale tidal motions. These are strongly forced in the nearfield of topography and their dissipation might represent a significant fraction of the energy lost at the Ridge. These motions will be studied in detail as an aspect of the Nearfield program. The reduction in energy experienced by these modes as they propagate to the farfield is a key measure of dissipation.

To resolve the higher mode motions, the Research Platform FLIP will be moored near the central tomography mooring, during the southern deployment of the array. Over a 30 day period the density (400 profiles/day with 1.5 m resolution) and velocity (720 profiles/day with 3 m resolution) fields will be sampled in the upper 800 m of the sea. Two CTDs and a lowered, up-down looking coded pulse Doppler sonar will obtain the measurements. Given the refraction associated with depth variation in the buoyancy frequency, the 800 m (0.2 ocean depth) is sufficient to distinguish modes 1 and 2 from 3 and 4, etc., but not sufficient to resolve individual modes. To improve resolution, a series of six temperature recorders will be placed on the nearby (~ 5 km) tomography mooring, at depths stretching from 800 m to the sea floor. These, combined with the FLIP measurements, yield the ability to distinguish the gravest few modes.

Figure F.4 illustrates Doppler sonar measurements of internal tide velocity (top) and shear (bottom) obtained in the 1986 Patchex Experiment. Note the extremely long vertical wavelength of the tidal velocity field and the slight hints of vertical phase propagation. The shear emphasizes the higher mode motions, giving clear signs of upward energy propagation (downward phase propagation) in the top 400 m early in the record. Such data, combined with corresponding density measurements, will be used to address the following issues:

- What is the modal content of the tidal signal in the farfield? How does the modal content compare with that in the nearfield? Are the higher modes lost? How does it compare with the non-tidal internal wave continuum?
- How does the wavenumber frequency spectrum of the wavefield compare with that as seen in the nearfield? With the G-M model?
- To what extent is the low wavenumber/high wavenumber motion coherent with astronomical forcing? How does this compare with the tomographic view of Dushaw *et al.* (1995) and the T/P view of Ray and Mitchum (1996)?
- What is the offshore energy flux? How does this compare with estimates derived from acoustic tomography? Is there a detectable flux divergence?
- How do offshore overturn rates compare with the nearfield, with TOGA COARE, with coastal California?

In addition, three temperature sensors distributed over the main thermocline on each of the other tomography moorings, as well as data from the HOT site (see Historical Data Analysis Program), will provide some information on the smaller-scale features in the farfield radiation at additional locations.

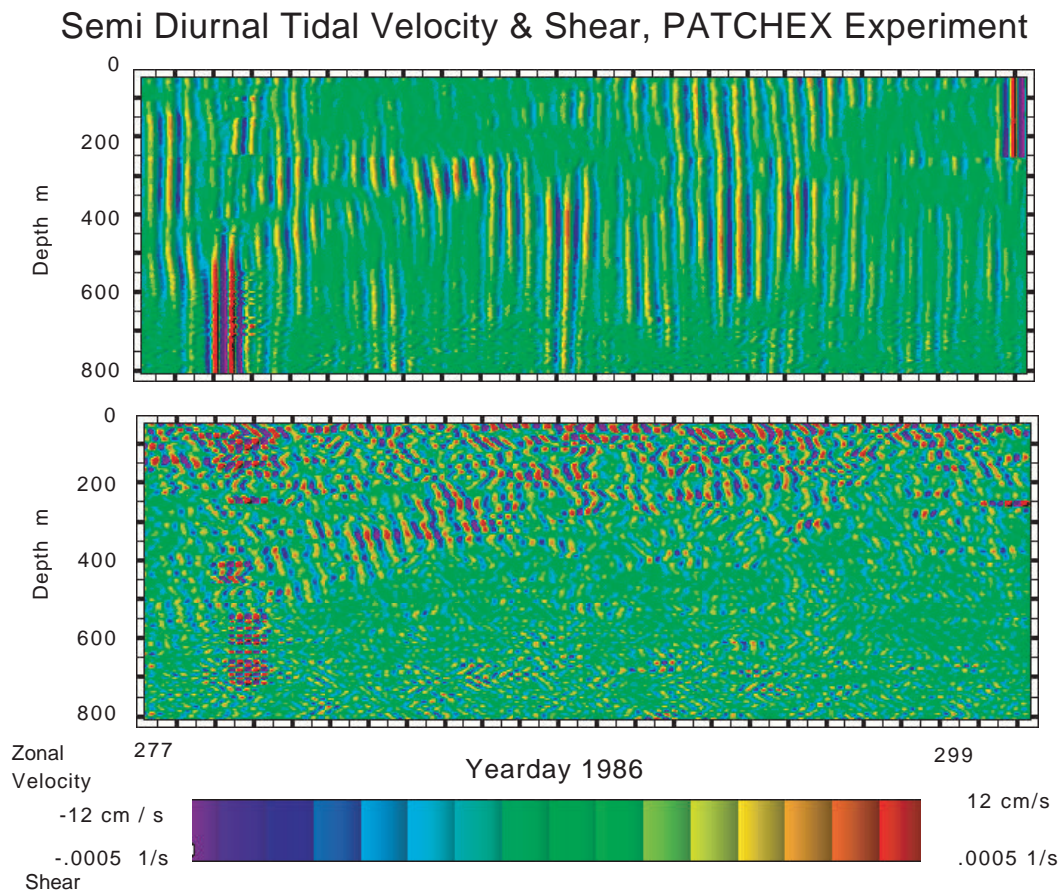


Figure F.4. Depth-time maps of semi-diurnal tidal velocity (top) and shear (bottom) obtained with a 75 kHz sonar mounted on the Research Platform FLIP. The vertical resolution of this sonar was 12 m.

5. ANALYSIS

Several current T/P tidal models consistently show that 20-30 GW of tidal energy is lost from the barotropic tide at the Hawaiian Ridge (Egbert, personal communication). This energy loss is roughly balanced by the radiating mode-1 baroclinic tides reported by Ray and Mitchum (1996). However, the HOT CTD time-series (CTD casts to 1000 m) suggests that mode-3 is dominant (Chiswell, 1994) so that higher-order modes in the farfield may constitute a significant amount of energy lost from the barotropic tide. In addition, an important conjecture of the HOME program is that the energy dissipated in the “nearfield” (e.g. within 10’s of km of the Ridge) is large compared to that radiated into the pelagic “farfield.” All of these results and speculations have significant uncertainties; the goal of the analysis of the farfield data is to determine all the components of the energy budget to far greater accuracy than is presently possible. These components are:

Barotropic tidal measurements and modeling. Gary Egbert has already implemented a preliminary regional barotropic tidal model for the Hawaiian Ridge over the area 180°-150° W, 15°-30° N on 900x490 grid. Preliminary runs of this model shows that currents, energy fluxes, and tidal dissipation at the Ridge are indeed sensitive to different drag parameterizations. Tidal currents parallel to the Ridge decrease by a factor of 3–4 and tidal dissipation increases by a factor of 5–6 when the drag coefficient is increased by an order of magnitude. (A substantial increase in drag coefficient is suggested since the T/P models appear to underestimate the energy lost at Hawaii.) This sensitivity shows that accurate measurements of barotropic tidal currents by tomography and HEM’s and tidal pressure by Pb’s are needed to better determine the drag parameterization in the tidal model, and hence better determine the barotropic tide energy flux convergence at the Ridge. The final analysis of these data will be an assimilation of them into the regional tidal model, a determination of the drag and/or mixing parameterization required for the model to best fit the data, and an accurate estimate of the barotropic tide energy flux convergence at Hawaii. The best dissipation parameterization may then be applied to the global ocean tide models.

Radiated baroclinic energy: Low mode. Tomography will be used to determine the low-mode energy radiated from the Ridge. The tomographic array is designed to provide good coverage of outward-going wavenumbers, so that very little low-mode energy will go unobserved.

Radiated baroclinic energy: High mode. The FLIP CTD data and Doppler sonar systems, together with the thermistor data obtained on the four tomography moorings and the CTD data obtained during HOT cruises, will be used to determine the modal content at six different points in the farfield. These data will determine the energy flux of both the higher-order modes and the spatially-incoherent components of the internal tidal field.

Nearfield dissipated energy. The remaining component of the energy budget is the nearfield dissipation. Thus, the combination of all results of the farfield experiment will determine the limits of energy available for local dissipation; this result may be used by the Nearfield program of HOME. All of these results set limits on the amount of energy lost from the barotropic tides that may be used for the maintenance of abyssal stratification. The results of these proposed process-oriented studies at Hawaii may then be used to better model tidal dissipation and internal-tide radiation in the global ocean.

REFERENCES CITED

- Chave, A.D. and D.S. Luther, 1990. Low-frequency, motionally induced electromagnetic fields in the ocean, 1, Theory, *J. Geophys. Res.*, **95**, 7185–7200.
- Chiswell, S.M., 1994. Vertical structure of the baroclinic tides in the central North Pacific subtropical gyre, *J. Phys. Oceanogr.*, **24**, 2032–2039.
- Dick, G., and G. Siedler, 1985. Barotropic tides in the Northeast Atlantic inferred from moored current meter data, *Deutsche Hydrographische Zeitschrift*, **38**, 7–22.
- Dushaw, B. D., B. D. Cornuelle, P. F. Worcester, B. M. Howe, and D. S. Luther, 1995. Barotropic and baroclinic tides in the central North Pacific Ocean determined from long-range reciprocal acoustic transmissions, *J. Phys. Oceanogr.*, **25**, 631–647.
- Dushaw, B. D., G. D. Egbert, P. F. Worcester, B. D. Cornuelle, B. M. Howe, and K. Metzger, 1997. A TOPEX/POSEIDON global tidal model (TPXO.2) and barotropic tidal currents determined from long-range acoustic transmissions, *Progr. Oceanogr.*, **40**, 337–367.
- Dushaw, B. D., and P. F. Worcester, 1998. Resonant diurnal internal tides in the North Atlantic, *Geophys. Res. Lett.*, **25**, 2189–2193.
- Dushaw, B. D., P. F. Worcester, B. D. Cornuelle, A. R. Marshall, B. M. Howe, S. Leach, J. A. Mercer, and R. C. Spindel, 1996. Data Report: Acoustic Mid-Ocean Dynamics Experiment (AMODE), Applied Physics Laboratory, University of Washington, APL-UW TM 2-96.
- Egbert, G. D., 1997. Tidal data inversion: Interpolation and inference, *Progr. Oceanogr.*, **40**, 53–80.
- Egbert, G. D., A. F. Bennett, and M. G. G. Foreman, 1994. TOPEX/POSEIDON tides estimated using a global inverse model, *J. Geophys. Res.*, **99**, 24821–24852.
- Filloux, J.H., D.S. Luther, and A.D. Chave, 1991. Update on seafloor pressure and electric field observations from the north-central and northeast Pacific: tides, infratidal fluctuations, and barotropic flow; in: Tidal Hydrodyn., B. Parker (Ed.), NY: John Wiley, 617–640.
- Luther, D.S., J.H. Filloux, and A.D. Chave, 1991. Low-frequency, motionally induced electromagnetic fields in the ocean, 2, Electric field and Eulerian current comparison from BEMPEX, *J. Geophys. Res.*, **96**, 12797–12814.
- Luyten, J. R., and H. M. Stommel, 1991. Comparison of M_2 tidal currents observed by some deep moored current meters with those of the Schwiderski and Laplace models, *Deep-Sea Res.*, **38**, S573–S589.

- Munk, W. H., 1997. Once again: once again—tidal friction, *Progr. Oceanogr.*, **40**, 7–35.
- Munk, W. H., and D. E. Cartwright, 1966. Tidal spectroscopy and prediction, *Phil. Trans. Roy. Soc., London*, **A259**, 533–581.
- Munk, W., P. Worcester, and C. Wunsch, 1995. *Ocean Acoustic Tomography*, Cambridge University Press, Cambridge, England, 433 pp..
- Munk, W. H., and C. Wunsch, 1997. The moon, of course... *Oceanography*, **10**, 132–134.
- Munk, W. H., and C. Wunsch, 1998. Abyssal recipes II: Energetics of tidal and wind mixing, *Deep-Sea Res.* (in press).
- Ray, R. D., and G. T. Mitchum, 1997. Surface manifestation of internal tides generated near Hawaii, *Geophys. Res. Lett.*, **23**, 2101–2104.
- Ray, R. D., and G. T. Mitchum, 1997. Surface manifestation of internal in the deep ocean: observation from altimetry and island gauges, *Prog. Oceanogr.*, **40**, 135–162.
- Samelson, R. M., 1998. Large-scale circulation with locally enhanced vertical mixing, *J. Phys. Oceanogr.*, **28**, 712–726.
- Sanford, T., 1971. Motionally-induced electric and magnetic fields in the sea, *J. Geophys. Res.*, **76**, 3476–3492.
- Schwiderski, E. W., 1979. Global ocean tides, Part II: The semidiurnal principal lunar tide (M_2), Atlas of Tidal Charts and Maps, N.S.W.C., TR79-414, Dahlgren, VA., 22448.
- Siedler, G. and U. Paul, 1991. Barotropic and baroclinic tidal currents in the eastern basins of the North Atlantic, *J. Geophys. Res.*, **96**, 22259–22271.
- Tierney, C. C., M. E. Parke, and G. H. Born, 1998. An investigation of ocean tides derived from along-track altimetry, *J. Geophys. Res.*, **103**, 10,273–10,287.
- Urlick, R. J., 1983. *Principles of Underwater Sound*, 3rd Edition, McGraw-Hill, New York.
- Wunsch, C., 1975. Internal tides in the ocean, *Rev. Geophys. Space Phys.*, **13**, 167–182.